Perturbation-response dynamics of coupled nonlinear systems

Cite as: Chaos 34, 103149 (2024); doi: 10.1063/5.0223294
Submitted: 13 June 2024 · Accepted: 8 October 2024 ·
Published Online: 29 October 2024

Georg Börner,[1,a)] Malte Schröder,[1] Moritz Thümler,[1] and Marc Timme[1,2,3,b)]

AFFILIATIONS

[1]Chair for Network Dynamics, Institute of Theoretical Physics and Center for Advancing Electronics Dresden (cfaed), TUD Dresden University of Technology, 01062 Dresden, Germany
[2]Center of Excellence Physics of Life, TUD Dresden University of Technology, 01062 Dresden, Germany
[3]Lakeside Labs, Lakeside B04b, 9020 Klagenfurt, Austria

Note: This paper is part of the Focus Issue, Nonautonomous dynamical systems: Theory, methods, and applications.
[a)]**Author to whom correspondence should be addressed:** georg.boerner@tu-dresden.de
[b)]**Email:** marc.timme@tu-dresden.de

ABSTRACT

How nonlinear systems dynamically respond to external perturbations essentially determines their function. Weak perturbations induce response dynamics near a stable operating point, often approximately characterized by linear response theory. However, stronger driving signals may induce genuinely nonlinear responses, including tipping transitions to qualitatively different dynamical states. Here, we analyze how inter-unit coupling impacts responses to periodic perturbations. We find that already in minimal systems of two identical and linearly coupled units, coupling impacts the dynamical responses in a distinct way. Any non-zero coupling strength extends the regime of non-tipping local responses relative to uncoupled units. Intriguingly, finite coupling may be more effective than infinitely strong coupling in keeping responses from tipping. Interestingly, already weak coupling may create novel response modes in strongly driven systems, implying the existence of multiple tipping points instead of only one. These results persist for systems of non-identical units, systems with nonlinear coupling, and larger networks of coupled units.

External perturbations continuously impinge on natural and engineered systems and may severely impact their functionality. How do complex nonlinear dynamical systems respond to time-dependent external fluctuations? Intriguingly, even weak coupling may enable novel localized response modes in strongly driven systems. However, for smaller, intermediate perturbation strengths, system responses may diverge. Overall, as the perturbation strength increases, the same system may undergo multiple tipping points, transitioning from localized to divergent, back to localized, and again to divergent responses. The observed phenomena robustly emerge across a broad range of system types, including systems of non-identical units, for nonlinear coupling, and in larger networks of units.

I. BACKGROUND

The collective nonlinear dynamics and reliable function of complex networked systems fundamentally underlie our daily lives, affecting systems as diverse as biological cells,[1] electric power grids,[2–4] and ecosystems.[5–7] Most natural and human-made complex systems are externally perturbed by driving signals that induce linear or nonlinear dynamical responses, including tipping, that disrupt the systems' intended or desired function.[8–12] While state-of-the-art theoretical concepts and method development have focused on linear responses suitable for weak driving signals,[8,13,14] it is far less understood how to characterize, predict, and design complex systems responding to strong perturbations.[15–18]

Here, we address the question of how coupling and fluctuating driving signals jointly impact nonlinear system responses. To obtain generic insights, we start by analyzing a minimal model of two identical units in which one periodically driven unit is linearly coupled to a second, unperturbed unit. We later illustrate how the results generalize to systems of non-identical units, larger networks, and nonlinear coupling.

In uncoupled systems, the driven unit exhibits periodic responses if driving signals are weak and undergoes tipping to diverging responses if the amplitude of the driving signals becomes

larger than a critical value. In the limit of infinitely strong coupling, both units respond identically and act like a single uncoupled unit subject to a perturbation signal of reduced strength. In contrast, intermediate coupling induces more intricate nonlinear response dynamics. In particular, non-diverging responses emerge beyond the critical perturbation strengths observed in both limiting cases. For strongly perturbed, weakly coupled systems, these responses constitute hybrid solutions where the driven variable experiences large excursions while the other stays closely localized in the vicinity of its stable operating point. Intriguingly, these systems exhibit multiple tipping points, where localized (non-diverging) system responses cease to exist, reemerge, and disappear again as the driving amplitude increases.

II. DRIVEN NONLINEAR COUPLED SYSTEMS

Consider a class of driven, networked dynamical systems of N units of the form

$$\dot{x}_i = f_i(x_i) + \sum_{j=1}^{N} h_{ij}(x_i, x_j) + \varepsilon\, g_i(t) \tag{1}$$

for $i \in \{1, \ldots, N\}$. Here, the functions $f_i : \mathbb{R} \to \mathbb{R}$ define the free (uncoupled) dynamics of the i-th unit. The functions $h_{ij} : \mathbb{R}^2 \to \mathbb{R}$ for $i \neq j$ and $h_{ii} = 0$ describe the pairwise interactions of unit j affecting unit i. The last term denotes the deterministic external driving signal $g_i(t)$ acting on unit i as a function of time t with a perturbation strength ε. In this work, we focus on periodic, single-frequency driving signals $g_i(t) = \delta_{i,k} \cos(\omega t)$, where k is the index of the driven variable and $\delta_{i,k}$ is the Kronecker delta. Without loss of generality we take $k = 1$ throughout.

For isolated driven units, recent research has uncovered genuinely nonlinear features of the dynamic response to deterministic periodic perturbations.[15] In contrast to the prediction of linear response theory, which suggests an oscillatory response around the original operating point for zero average driving, asymmetries in the internal dynamics cause a shift of the average response. This offset $\Delta\bar{x} \sim \varepsilon^2$ is an intrinsically nonlinear effect [see also Eqs. (4a) and (4b) and Fig. 2(a)] and emerges already for arbitrarily small driving forces ε. Recent work also presented a method to estimate the critical amplitude above which responses no longer stay local but diverge.[15]

How does coupling among several units affect such nonlinear responses? To isolate the impact of coupling from the topology of the interaction network, we start by analyzing a minimal model of $N = 2$ identical units with linear coupling, where one unit is subject to deterministic driving [Fig. 1(a)]. Equation (1) becomes

$$\dot{x} = f(x) + \beta(y - x) + \varepsilon \cos(\omega t) \tag{2a}$$

$$\dot{y} = f(y) + \beta(x - y), \tag{2b}$$

where we simplified notation to $x = x_1$ and $y = x_2$. The two parameters β and ε denote the coupling strength and the perturbation strength, respectively. Rescaling time, we set $\omega = \pi$ without loss of generality and consider free dynamics defined by

$$f(x) = \begin{cases} \alpha - \cos(x) & \text{for } |x| < \pi \\ 1 + \alpha & \text{else,} \end{cases} \tag{3}$$

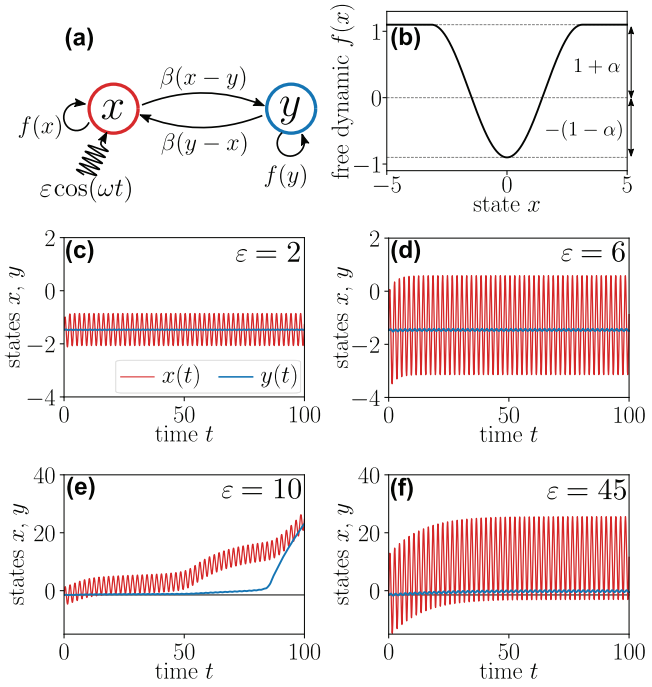

FIG. 1. Multiple tipping points separate localized and diverging response dynamics. (a) Scheme illustrating the system of two coupled units [Eqs. (2a) and (2b)]. (b) Function $f(x)$ [Eq. (3)] that determines free (uncoupled, unperturbed) dynamics. (c)–(f) Dynamic responses $x(t)$ of the driven unit (red) and $y(t)$ of the unperturbed second unit (blue) for different perturbation strengths ε. (c) and (d) For sufficiently weak perturbations, both $x(t)$ and $y(t)$ oscillate approximately around the fixed point of the unperturbed system and the response amplitude increases with the perturbation strength. (e) Once ε has passed a critical value, the response dynamics becomes unstable and both units continually drift towards higher values. (f) For even stronger perturbations, stationary response dynamics reemerges. The driven variable $x(t)$ oscillates with a large offset and an average response far outside the basin of attraction of the stable operating point of the unperturbed system while the second variable $y(t)$ oscillates within the basin of attraction. Model Parameters: Eqs. (2a) and (2b), with asymmetry parameter $\alpha = 0.1$, coupling strength $\beta = 0.075$, initial conditions $x(0) = y(0) = x_s^*$.

with $\alpha > 0$ set to $\alpha = 0.1$ if not specified otherwise [Fig. 1(b)]. The free dynamics exhibit one stable operating point at $x_s^* = -\arccos\alpha$ which we take as initial condition in all simulations. An unstable fixed point at $x_u^* = \arccos\alpha$ and $f(x) > 0$ for sufficiently large $|x|$ ensures that the system exhibits diverging responses, $x(t) \to \infty$ for $t \to \infty$, for strong perturbations. A more detailed overview of the fixed points of the coupled system is provided in the Appendix and illustrated in Fig. 5.

This simplified model setting ensures that the observed nonlinear responses are only affected by the coupling between the units, not by heterogeneities among the units, nonlinearities in the coupling, stochasticity of the driving signal, the topology of the coupling among units, or some collective response mode potentially arising in systems with many units. In particular, we also avoid system-intrinsic dynamical phenomena such as a finite-time blowup as arising, e.g., for free dynamics of normal form[14] $f(x) = x^2 - \alpha$. As we

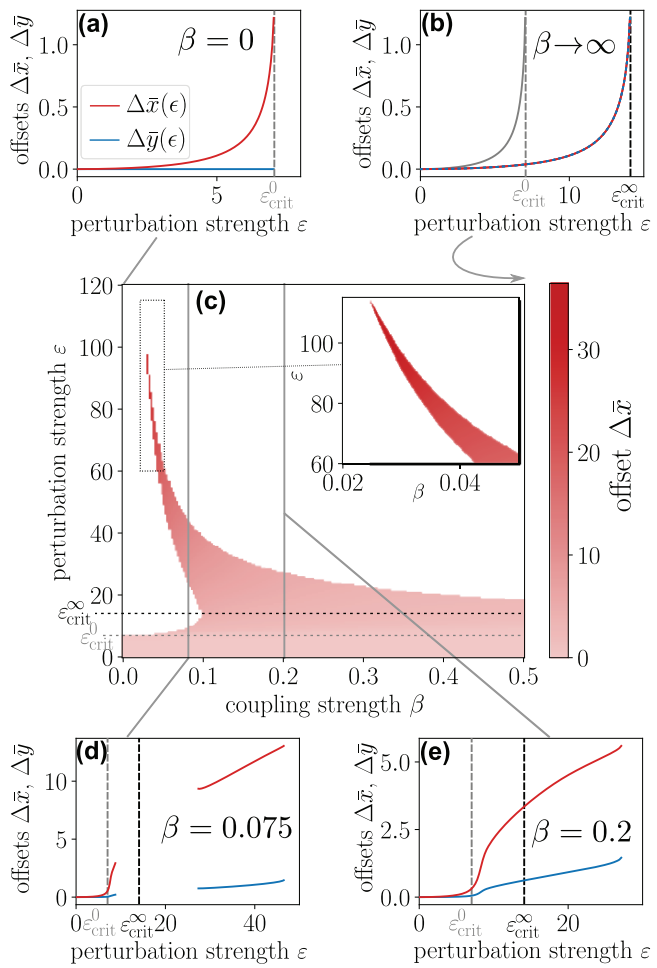

FIG. 2. Weak coupling induces localized average responses to strong perturbations. (a) Nonlinear offsets $\Delta\bar{x}$ and $\Delta\bar{y}$ for uncoupled units, $\beta = 0$. Only the driven unit's variable x responds to the perturbation, with an offset $\Delta\bar{x}(\varepsilon)$ that increases nonlinearly with the perturbation strength ε until the response diverges for $\varepsilon > \varepsilon^{(0)}_{\text{crit}}$ (dashed vertical line). (b) In the limit of strong coupling, $\beta \to \infty$, both units x and y react identically to the perturbation, like a one-dimensional system affected by a perturbation of strength $\varepsilon/2$ [Eq. (7)], with a critical coupling strength $\varepsilon^{(\infty)}_{\text{crit}} = 2\varepsilon^{(0)}_{\text{crit}}$ (dashed vertical line, compare gray lines for the uncoupled dynamics). (c) Nonlinear offset $\Delta\bar{x}$ of the driven unit color coded (shades of red), as a function of the coupling strength β and the perturbation strength ε. White denotes diverging responses without a finite offset $\Delta\bar{x}$. For small positive coupling strengths β, responses also exist beyond the limiting critical coupling strengths (dashed horizontal lines), up to $\varepsilon \approx 112$ (see the inset). For small coupling strengths β, multiple transitions exist between localized and divergent responses as the perturbations get stronger (compare panel d). (d) and (e) Nonlinear offsets $\Delta\bar{x}$ and $\Delta\bar{y}$ for coupling strengths $\beta = 0.075$ and $\beta = 0.2$, respectively [compare gray vertical lines in panel (c)]. For both coupling strengths, localized average responses exist beyond the limiting critical perturbation strengths $\varepsilon^{(0)}_{\text{crit}}$ and $\varepsilon^{(\infty)}_{\text{crit}}$. However, for weak coupling, the response diverges at intermediate perturbation strengths [gap of both lines in panel (c)]. Model parameters as in Fig. 1, Eqs. (2a) and (2b), $\alpha = 0.1$, driving frequency $\omega = \pi$, and initial conditions $x(0) = y(0) = x^*_s$.

report below, the core phenomena persist also for other choices of the intrinsic dynamics of the units, for nonlinearly coupled units, for systems of non-identical units, and for larger networks of units.

III. NONLINEAR RESPONSES OF COUPLED UNITS

Trajectories from direct numerical integration for small coupling strength β provide an overview of possible response dynamics as the perturbation amplitude increases [Figs. 1(c)–1(f)]. Both units oscillate in response to the periodic driving, with the directly driven unit responding more strongly. For weak coupling, both units oscillate approximately around the stable operating point of their intrinsic dynamics. As the perturbation strength ε increases, the response amplitude increases until, beyond a critical perturbation strength $\varepsilon^{(\beta)}_{\text{crit}}$, the response becomes unstable and diverges. This form of tipping upon increasing the driving amplitude resembles the response dynamics recently explained and quantitatively estimated for one-dimensional systems.[15] Intriguingly, for even larger perturbation strengths, a stationary (non-diverging) response reemerges with hybrid dynamics of both units [Fig. 1(f)]. The driven variable $x(t)$ oscillates with a large amplitude around an average value far away from its original stable operating point and outside of its basin of attraction, while the second variable $y(t)$ oscillates only weakly with a slight offset within the basin of attraction of its (one-dimensional) stable fixed point. For even stronger perturbations (not shown here), again the responses diverge, albeit faster than those for intermediate perturbation strengths [see Fig. 1(e)]. This is ultimately the expected behavior for any large-amplitude perturbation [see Figs. 2(c) and 2(d) for an illustration].

In contrast to the one-dimensional system, we, thus, observe not one tipping point at one critical driving amplitude— instead the coupling between units induces multiple tipping transitions.

We quantitatively characterize the response dynamics by the offset,

$$\Delta\bar{x} = \lim_{t_1 \to \infty} \frac{1}{T} \int_{t_1}^{t_1+T} x(t)\,\mathrm{d}t - x^* \tag{4a}$$

$$\Delta\bar{y} = \lim_{t_1 \to \infty} \frac{1}{T} \int_{t_1}^{t_1+T} y(t)\,\mathrm{d}t - y^* \tag{4b}$$

defined as the deviation of the long-term average response over a period $T = 2\pi/\omega$ of the perturbation signal from the original operating state, similar to Ref. 15. By taking the limit $t_1 \to \infty$, we ignore transient times. In contrast to predictions from linear response theory,[2] the averages of the nonlinear response dynamics generally feature non-zero offsets, $\Delta\bar{x} \neq 0$ and $\Delta\bar{y} \neq 0$, from the original fixed point.

IV. WEAK-COUPLING AND STRONG-COUPLING LIMITS

In the limit of uncoupled units and in the limit of infinitely strong coupling, the system dynamics reduce to those of a single driven unit.

For uncoupled units, $\beta = 0$, the dynamical equations (2a) and (2b) are given by

$$\dot{x} = f(x) + \varepsilon \cos(\omega t), \tag{5a}$$

$$\dot{y} = f(y). \tag{5b}$$

The time-dependent perturbation of the variable x does not affect variable y and the response dynamics are characterized by the single one-dimensional differential equation (5a) for the driven unit x. As expected from previous research,[15] the system exhibits stable oscillatory responses for weak perturbation strengths with a nonlinear offset $\Delta\bar{x} = \mathcal{O}(\varepsilon^2)$ as $\varepsilon \to 0$. Beyond some critical perturbation strength $\varepsilon_{\text{crit}}^{(0)}$, the responses diverge such that $\Delta\bar{x}$ is not finite [Fig. 2(a)].

In the strong-coupling limit $\beta \to \infty$, both units respond exactly in unison. Expressing the dynamics of x and y in terms of a center-of-mass coordinate $u = (x + y)/2$ and a relative coordinate, $v = (x - y)/2$, the dynamical equations (2a) and (2b) become

$$\dot{u} = \frac{1}{2}\left(f(x) + f(y) + \varepsilon \cos(\omega t)\right), \tag{6a}$$

$$\dot{v} = \frac{1}{2}\left(f(x) - f(y) + \varepsilon \cos(\omega t)\right) - \beta\, v. \tag{6b}$$

As $\beta \to \infty$, the coupling term dominates the time derivative $\dot{v}$, overruling the intrinsic dynamics of the units and the perturbation such that $v(t) \to 0$ as $t \to \infty$. Together with the identical initial conditions of both units, $x(0) = y(0)$, this gives a constant difference $v(t) = x(t) - y(t) = 0$. The time evolution of the center-of-mass coordinate $u = x = y$ then reduces to

$$\dot{u} = f(u) + \frac{\varepsilon}{2} \cos(\omega t) \tag{7}$$

and follows the one-dimensional dynamics of a single (uncoupled) unit with a reduced effective perturbation strength $\varepsilon/2$. The system, thus, responds qualitatively identically to the uncoupled driven unit with a perturbation strength reduced by a factor of two. Importantly, the response remains non-diverging up to a critical perturbation strength $\varepsilon_{\text{crit}}^{(\infty)}$ twice as large as in the uncoupled case,

$$\varepsilon_{\text{crit}}^{(\infty)} = 2\varepsilon_{\text{crit}}^{(0)}, \tag{8}$$

see Fig. 2(b).

V. LOCALIZED RESPONSES TO LARGE PERTURBATIONS

Intriguingly, for intermediate coupling β, the critical perturbation amplitude does not monotonically increase. Localized responses to large perturbations exist also beyond the critical perturbation strengths $\varepsilon_{\text{crit}}^{(0)}$ and $\varepsilon_{\text{crit}}^{(\infty)}$ of the two limiting cases considered above. Figure 2(c) illustrates the parameter region in the β-ε-space where localized responses exist, characterized by a finite nonlinear offset $\Delta\bar{x}(\beta, \varepsilon)$ of the driven unit. For a wide range of $\beta > 0$, the system exhibits localized response dynamics also for perturbation strengths $\varepsilon > \varepsilon_{\text{crit}}^{(\infty)}$, even up to large perturbation strengths $\varepsilon \approx 112$. However, for $\beta \lesssim 0.1$, localized dynamics may cease to exist for intermediate perturbation strengths ε, such that there is not a single unique critical perturbation strength but multiple transitions from localized to divergent, to localized, and finally again to divergent responses. In the upper branch of localized responses for large perturbation strengths ε, the response dynamics exhibit a large offset of the driven unit [Fig. 2(d)], indicating the hybrid response observed in Fig. 1(f).

VI. ORIGIN OF LOCALIZED RESPONSE DYNAMICS

How do these localized dynamics far from the stable operating point of the unperturbed system emerge? We first consider the fixed point structure of the coupled system in a simpler case, taking the parameter $\alpha = 0$ for the intrinsic dynamics equation (3) [compare Fig. 1(b)]. The system has two symmetric fixed points from the uncoupled system $x_s^* = y_s^* = -\arccos\alpha$ (stable) and $x_u^* = y_u^* = \arccos\alpha$ (unstable). For sufficiently weak coupling, the system also has additional asymmetric fixed points. One of these fixed points is $x^{**} = 1/\beta$ and $y^{**} = 0$ which exists for $\beta < 1/\pi$. The intrinsic dynamics push both units in opposite directions, $f(x^{**}) = 1$ and $f(y^{**}) = -1$. However, the coupling $\beta\,(y^{**} - x^{**}) = -1$ between the units exactly cancels the intrinsic force. This fixed point also exists (at different values) for $\alpha < 0$ and annihilates in a saddle-node bifurcation[19] exactly at $\alpha = 0$ (see the Appendix and Fig. 5 for a more detailed overview of the fixed points and bifurcations in the system). The hybrid responses for $\alpha > 0$ are a ghost of this stable fixed point.

As a necessary condition for the existence of a periodic response that is non-divergent and in this sense localized, the average force from the intrinsic dynamics and the coupling have to cancel out over one period of the driving signal. Figure 3 illustrates the three qualitatively different types of responses. For small perturbation strengths ε, the system oscillates around the stable operating state (x_s^*, y_s^*) [Fig. 3(a)]. In this state, the force from the intrinsic dynamics of the units approximately averages out individually, even without the coupling [Fig. 3(b)].

In contrast, for large perturbation strengths ε, the units exhibit hybrid responses, oscillating around the ghost fixed point at $(x^{**}, y^{**}) = (1/\beta, 0)$ [Fig. 3(c)]. The response amplitude of the driven unit is sufficiently large that the system returns to the basin of attraction of the original operating state. The intrinsic force of both units does not average to zero over one period of the response. However, the driven unit returns to the basin of attraction of the original operating state where $f(x) < 0$, reducing the average force from $f(x^{**}) = 1 + \alpha$ to $\overline{f(x)} < 1 - \alpha$. The second unit oscillates close to the minimum of $f(y)$ such that $\overline{f(y)} = -\overline{f(x)}$. The coupling between the units is, thus, able to counteract the opposing forces of the intrinsic dynamics and stabilize hybrid responses oscillating around or near the ghost fixed point (x^{**}, y^{**}) [Fig. 3(d)].

For intermediate perturbation strengths ε, the oscillations of the system also tend toward the ghost fixed point (x^{**}, y^{**}) [Fig. 3(e)]. However, due to the smaller perturbation strength, the response amplitude of the driven unit is not large enough for it to reach the basin of attraction of its original operating state. The average force is $\overline{f(x)} \approx 1 + \alpha > 1 - \alpha$ such that the second unit cannot compensate the intrinsic force, because $\overline{f(y)} > -(1 - \alpha)$, even if it

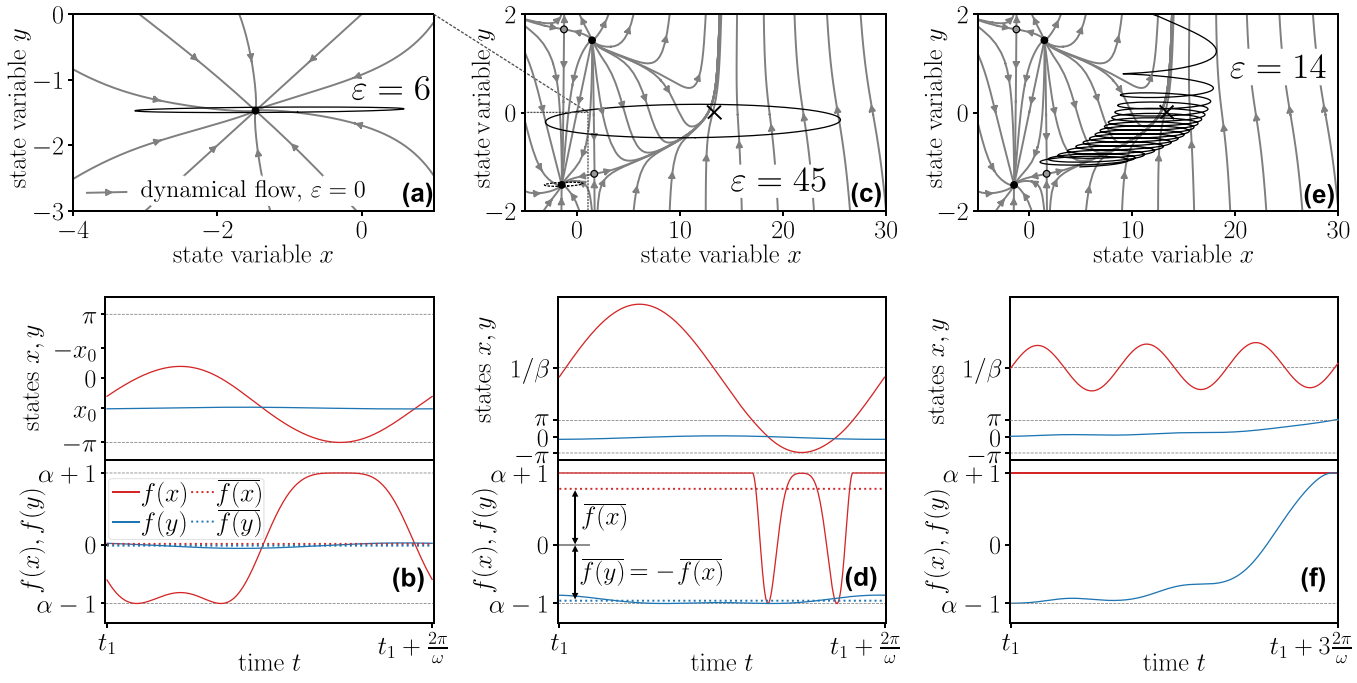

FIG. 3. Force balance at ghost fixed point explains localized responses for large perturbations. (a) For weak perturbations, $\varepsilon = 6$, both units oscillate around the localized operating point (x_s^*, y_s^*). Arrows represent the dynamical flow of the unperturbed system. (b) Over one period of the response, the average forces from the intrinsic dynamics of both units approximately cancels even without the coupling, $\overline{f(x)} \approx 0$ and $\overline{f(y)} \approx 0$ (dotted lines). (c) For strong perturbations, $\varepsilon = 45$, the units oscillate around the ghost fixed point $(x^{**}, y^{**}) = (1/\beta, 0)$ (cross). For comparison, the dashed rectangle and the dashed ellipse recall the state space region and the system's response shown in panel (a). (d) The response of the driven unit (red) reaches into the basin of attraction of the original operating point where $f(x) < 0$, reducing the average force of the intrinsic dynamics. The average force on both units becomes equal in magnitude, $\overline{f(x)} = -\overline{f(y)} < 1 - \alpha$ (dotted lines), such that the coupling is able to stabilize the opposing intrinsic forces. (e) For intermediate perturbation strengths, $\varepsilon = 14$, the response slowly drifts along the unstable manifold of the saddle point (open circle). (f) Due to the weaker perturbation, the response amplitude of the driven unit is too small to reach the basin of attraction of the original operating point. The average force is $\overline{f(x)} > 1 - \alpha > -\overline{f(y)}$ such that the system overall slowly drifts towards larger values and eventually diverges.

remained at the minimum (and, thus, extremum) of $f(y)$ without oscillating. The response slowly drifts along the unstable manifold of the remaining saddle point and passes the ghost fixed point as it diverges [Fig. 3(f), compare Fig. 1(f)].

VII. ROBUSTNESS OF RESPONSE DYNAMICS

The reported phenomena are robust and generalize to systems of non-identical units, nonlinear coupling, and larger networks of units. Indeed, the core qualitative arguments presented above also hold in such more intricate settings.

In particular, the same qualitative state space and bifurcation structure persist for symmetric local forces ($\alpha = 0$) and for reversed asymmetry [$\alpha < 0$, Fig. 4(a)]. For symmetric local forces, the upper branch of the localized response regime diverges, $\varepsilon_{\text{crit}} \to \infty$ as $\beta \to 0$. As a consequence, localized responses exist for arbitrarily large perturbation amplitudes ε and for arbitrarily small coupling strengths β. For reversed asymmetry, $\alpha < 0$, the ghost becomes a real fixed point through a reverse saddle-node bifurcation, enabling the same localized response (compare also Fig. 5 in the Appendix). In addition, the intrinsic dynamics are now shifted such that the unperturbed unit can always counteract the intrinsic force experienced by the other unit [compare Figs. 3(c) and 3(d)]. For small coupling strengths β, a second branch of stable oscillatory responses becomes possible around the stable asymmetric fixed point. These solutions never reach the basin of attraction of the original operating point or the unstable asymmetric fixed point [compare Figs. 5(g)–5(i)].

The same qualitative dynamics emerge for quantitatively modified intrinsic dynamics of the units, including asymmetric dynamics $f(x) \neq f(-x)$ [Fig. 4(b)] and non-identical units [Fig. 4(c)].

Similar localized responses may also emerge for qualitatively different, unbounded intrinsic dynamics, $f(x) \sim a\,x^2 \to \infty$ for $|x| \to \infty$ [Figs. 4(d)–4(f)]. If the intrinsic force remains small, the dynamics are qualitatively identical to the previous observations [Fig. 4(d)]. For larger intrinsic forcing, the parameter region allowing stable localized responses no longer folds back to small coupling strengths β and only a single tipping point exists for a given coupling. However, stable localized responses may still exist for significantly larger perturbation strengths [Fig. 4(e)]. If the force from the intrinsic dynamics becomes too large, localized responses are only possible for oscillations within or very close to the basin of

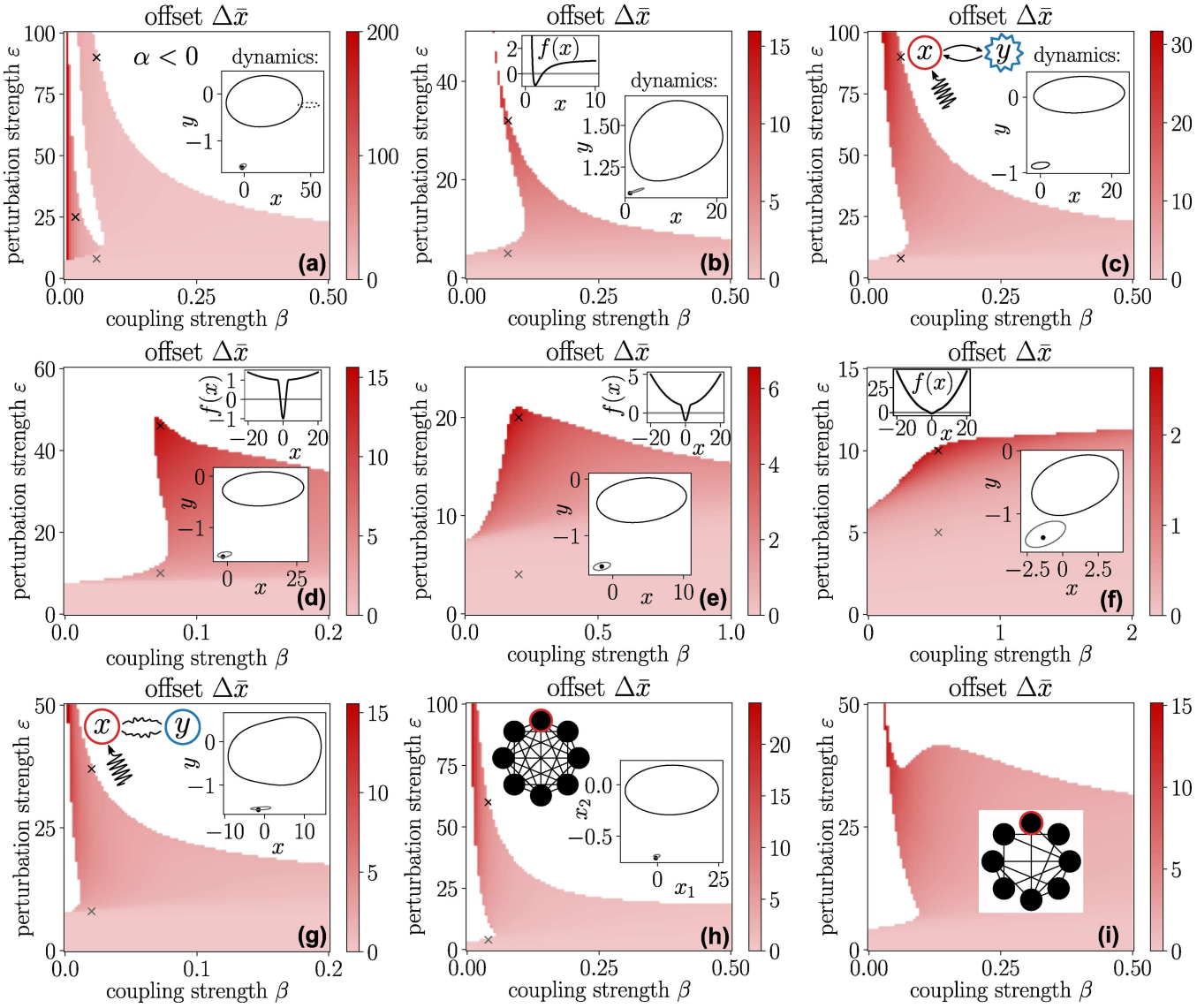

FIG. 4. Localized hybrid responses robustly emerge across a variety of systems. Panels show the average offset $\Delta\bar{x}$ as a function of coupling strength β and perturbation strength ε [as Fig. 1(c)] for various generalizations of the system studied extensively above. Insets illustrate the model setting and typical localized dynamics together with the unperturbed operating point at selected parameters (crosses in the main panels), respectively. For all variations, the qualitative dynamics remain largely robust and similar to the minimal model system. (a) Identical two-unit system as defined by Eqs. (2a), (2b), and (3) at $\alpha = -0.001$. (b) Identical two-unit system as defined by Eqs. (2a) and (2b), with $f(x) = 8x^{-2}(x^{-2} - 1) + 1.1$. (c) Heterogeneous 2-unit system with $f_x(x) = f(x; \alpha_x)$ and $f_y(y) = f(y - 0.3; \alpha_y)$ following Eq. (3) with different parameters $\alpha_x = 0$ and $f(y)$ with $\alpha_y = 0.3$. Here, the offset $\Delta\bar{x}$ is defined relative to the fixed point of the uncoupled system. (d)–(f) Identical two-unit system as defined by Eqs. (2a) and (2b), with $f(x)$ as given in Eq. (3) with $\alpha = 0$, modified as $f(x) \to f(x) + ax^2$, with $a = 0.001$ (panel d), $a = 0.01$ (panel e), and $a = 0.1$ (panel f). (g) Identical 2-unit system with nonlinear coupling function $h_{1,2}(x, y) = (y - x)^3/|y - x|$. (h) All-to-all network of $N = 8$ identical units, with $f(x_n)$ as in Eq. (3) and $\alpha = (N - 2)/N = 0.75$. At this value of α, a saddle point emerges at $(x_1, x_2, \ldots, x_N)^T = (2/(\beta N), 0, \ldots, 0)^T$, where a single strongly deflected unit x_1 is exactly balanced by the other units. This corresponds to symmetric local dynamics, $\alpha = 0$, in the minimal model setting. (i) Connected random network (drawn from Gilbert ensemble at $p = 0.5$), with $N = 8$ identical units and $f(x_n)$ as in Eq. (3) with $\alpha = 0.65$.

attraction of the original operating point. The critical perturbation strength ε^* increases monotonically with the coupling strength β [Fig. 4(f)].

Even for qualitatively modified coupling between the units, the observed dynamics remain robust. This includes systems with nonlinear coupling [Fig. 4(g)], all-to-all coupled networks of $N >$

2 units [Fig. 4(h)], and networks with random coupling topology [Fig. 4(i)].

VIII. CONCLUSIONS

The influence of external time-dependent signals on dynamical systems is often quantified by linear response theory.[3,8,13,14,20–22] Recent work[15] has reported genuinely nonlinear responses to periodic perturbations resulting in a non-zero average offset away from the stable operating point of a system. The offset predicts qualitative changes in the response dynamics when the system undergoes tipping for sufficiently strong perturbations and the response diverges. Although such nonlinear offsets and tipping have been equally observed for coupled networked systems of several variables, the impact of inter-variable coupling on such responses has remained unclear so far.

However, the impact of coupling on these nonlinear response dynamics is highly non-trivial. We find that for weak coupling, two parameter regions of localized responses exist, one for sufficiently small perturbation amplitude and a second for large perturbations beyond the expected critical perturbation strength for uncoupled or strongly coupled units. In this second regime, the system exhibits hybrid periodic responses and oscillates around a ghost fixed point far away from the original operating point. The driven variable responds with large-amplitude oscillations and a large average offset, whereas the coupled variable responds with periodic low-amplitude excursions within the basin of attraction of its stable operating point. If the driving amplitude is in between these two regimes or too large, responses diverge over time. Instead of a single critical perturbation strength ε_c, a total of three transitions emerge with increasing perturbation strength. With increasingly strong coupling, these two response modes merge such that periodic low-amplitude responses prevail for sufficiently weak driving and responses diverge above a critical perturbation strength ε_c. These phenomena are robust with respect to varying intrinsic unit dynamics and coupling functions and equally emerge in larger networks, also with intricate coupling topologies.

Our results underline the intricate joint impact of inter-variable coupling and external driving on the collective response properties of driven nonlinear dynamical systems. Interestingly, already (arbitrarily) weak coupling might allow for more effective absorption of external, fluctuating perturbations *on average*. Despite the weak average deviation, coupling enables substantial temporary deviations from an original fixed point. Indeed, we may view the fluctuating driving signal as stabilizing responses that on average are located near a previously existing fixed point (ghost) of the system dynamics.

Future work needs to more systematically address responses of networked systems of coupled nonlinear units. As initial candidate network topologies, representatives of spatially extended systems, like cycle graphs, chains, or lattices, and globally coupled systems or small motif networks constitute the most immediate generalizations of the two-variable systems considered here. Whereas the results reported above open up novel perspectives on potential collective response dynamics emerging through coupling, we are still missing a systematic understanding of how coupling controls possible responses. Furthermore, it remains unknown under which conditions new forms of collective responses may emerge. Open questions include, for instance, how responses of different units interfere in multi-variable systems and how systems respond to driving signals perturbing more than one variable.

Our theoretical results may find key applications in several fields. For instance, ecosystems that are periodically driven may respond in unexpected ways.[7,23] The eutrophication of lakes driven by noisy, roughly periodic signals exhibit tipping points[24] one may want to predict in model settings by combining insights from[15] with results reported above. It also remains an open question how to mitigate dysfunction—for example, voltage drops or power outages—in electric power grids that are driven by fluctuating renewable-source inputs[4,25] or fluctuating demand.[26] Furthermore, climate systems as representatives of highly interconnected complex systems are often periodically driven and it still is a challenge to predict their responses.[27]

Because generic nonlinearly shifted periodic responses as well as the tipping transition itself constitute genuinely nonlinear phenomena, responses from different driven units in the same system do not superimpose linearly, not even at arbitrarily small driving amplitudes. Nonlinear response phenomena of fluctuation-driven systems thus require their own dedicated branch of analysis to understand emerging response patterns, in turn needing the development of suitable mathematical tools appropriate for networked dynamical systems that are driven and respond in a genuinely nonlinear fashion.

ACKNOWLEDGMENTS

We thank Frank Jülicher for valuable discussions on coupled non-autonomous systems. Partially funded by the Bundesministerium für Bildung und Forschung (BMBF, Federal Ministry of Education and Research) under Grant. No. 03SF0769 and by the Deutsche Forschungsgemeinschaft (DFG, German Research Foundation) under Germany's Excellence Strategy—EXC-2068—390729961 (Cluster of Excellence Physics of Life).

AUTHOR DECLARATIONS

Conflict of Interest

The authors have no conflicts to disclose.

Author Contributions

Georg Börner: Conceptualization (lead); Data curation (lead); Formal analysis (lead); Investigation (lead); Methodology (equal); Software (lead); Validation (equal); Visualization (lead); Writing – original draft (lead); Writing – review & editing (lead). **Malte Schröder:** Conceptualization (equal); Formal analysis (equal); Investigation (equal); Methodology (equal); Supervision (equal); Validation (supporting); Writing – original draft (equal); Writing – review & editing (equal). **Moritz Thümler:** Conceptualization (equal); Investigation (supporting); Methodology (equal); Supervision (supporting); Writing – original draft (equal); Writing – review & editing (equal). **Marc Timme:** Conceptualization (equal); Funding acquisition (lead); Investigation (supporting); Methodology (equal);

Project administration (lead); Supervision (equal); Validation (supporting); Writing – original draft (equal); Writing – review & editing (equal).

DATA AVAILABILITY

The data that support the findings of this study are available from the corresponding author upon reasonable request.

APPENDIX: FIXED POINT ANALYSIS FOR SMALL $\beta > 0$

The dynamics of the model system discussed in the main text depends on its fixed point structure. With the internal dynamics as given by Eq. (3), for all $\alpha \in (-1, 1)$ and $\beta \in [0, \infty)$, there is a stable operating point $(x_s^*, y_s^*)^\mathsf{T} = (-\arccos\alpha, -\arccos\alpha)^\mathsf{T}$. As discussed in Sec. VI, for sufficiently weak periodic driving (small ε), the collective dynamics stays in the vicinity of this stable fixed point, as predicted also by linear response theory. Then, the forces $f(x)$ and $f(y)$ (approximately) cancel out over one period of the perturbation, $\overline{f(x)} \approx 0$, $\overline{f(y)} \approx 0$, so that each variable x, y is stable by itself [compare Figs. 3(a) and 3(b)].

In this region of state space, the dynamics are dominated by two fixed points (one stable and one unstable) of the individual one-dimensional intrinsic dynamics where $f(x) = 0$. In the coupled system, four fixed points exist close to combinations of the stable and unstable fixed point of these one-dimensional dynamics [Figs. 5(a)–5(c)]: two symmetric fixed points at $(x_s^*, y_s^*)^\mathsf{T} = (-\arccos\alpha, -\arccos\alpha)^\mathsf{T}$ (stable) and $(x_u^*, y_u^*)^\mathsf{T} = (\arccos\alpha, \arccos\alpha)^\mathsf{T}$ (unstable) and two asymmetric fixed points close to $(x_s^*, y_u^*)^\mathsf{T} \approx (-\arccos\alpha, \arccos\alpha)^\mathsf{T}$ and

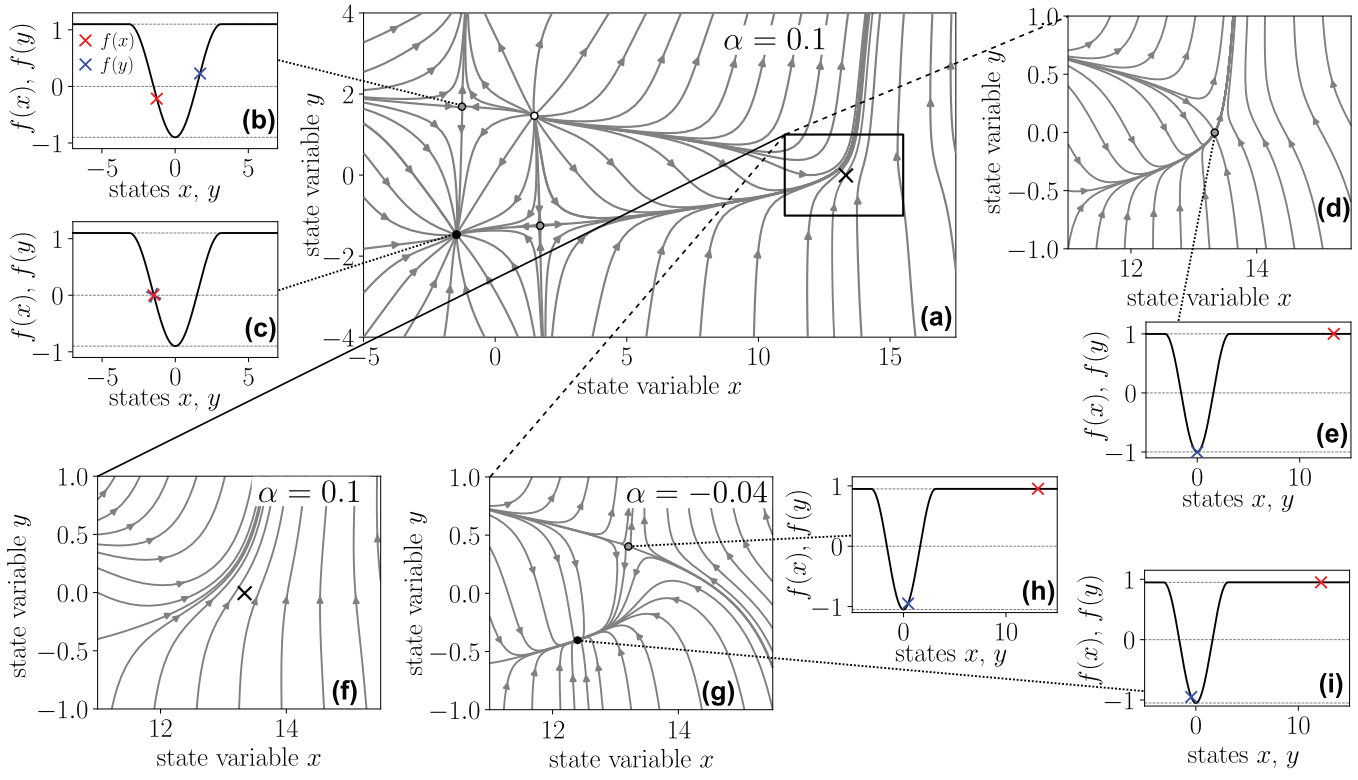

FIG. 5. Ghost fixed point determines the structure of the dynamical flow. (a) Portrait of the dynamical flow and relevant fixed points of the coupled two-unit system defined by Eqs. (2a), (2b), and (3) for $\alpha = 0.1$ and $\beta = 0.075$. (b) and (c) Schematic illustration of two of the four fixed points close to combinations of the fixed points of the intrinsic dynamics where $f(x) = 0$. Panel (c) illustrates the stable operating point $(-\arccos\alpha, -\arccos\alpha)^\mathsf{T}$. (d) Zoom-in for large x, with $\alpha = 0$. For this parameter choice, a saddle point exists at $(1/\beta, 0)$. It has a stable and a (linearly) neutrally stable manifold such that the dynamical flow is qualitatively similar to the case with $\alpha > 0$ [panels (a) and (f), the last position of the saddle point is marked by the black cross]. (e) Schematic illustration of the asymmetric saddle point. Note that $f(x) = -f(y)$ so that the overall forces on both units are exactly canceled out by the coupling. (f) For $\alpha > 0$ [as in panel (a)], the system does not exhibit a fixed point for large x, but the unstable manifolds from two existing fixed points for smaller x still converge to the same trajectory. The overall flow remains similar due to the ghost of a fixed point existing at $\alpha = 0$ (black cross). (g) For $\alpha < 0$, a saddle-node bifurcation gives rise to a stable fixed point and a saddle point. Note that globally, apart from the small region between the two fixed points, the dynamical flow still remains similar [compare response dynamics illustrated in Fig. 4(a)]. (h) and (i) Schematic illustration of the two fixed points emerging from the saddle-node bifurcation.

$(x_u^*, y_s^*)^T \approx (\arccos\alpha, -\arccos\alpha)^T$ (both unstable). For $\alpha > 0$ and sufficiently small coupling strength $\beta < 1/\pi$, these are the only four fixed points.

For larger perturbation strengths ε, generally the collective response leaves the basin of attraction of the stable operating point $(x_s^*, y_s^*)^T$ and the dynamics in other parts of state space becomes relevant. However, for $\alpha > 0$, the emergence of non-divergent collective responses cannot be directly linked to a fixed point of the unperturbed system. Instead, the response is determined by the dynamical flow along the unstable manifold of the saddle $(x_u^*, y_s^*)^T \approx (\arccos\alpha, -\arccos\alpha)^T$, which converges to the same trajectory as the unstable manifold of the symmetric unstable fixed point for large x [Fig. 5(d)].

This structure represents the remains of strongly asymmetric fixed points that undergo a saddle-node bifurcation[19] at $\alpha = 0$. Exactly at $\alpha = 0$, there is a saddle point $(1/\beta, 0)^T$, where the intrinsic forces on both units, $f(x) = -f(y) = 1$, are exactly balanced by the forces of the inter-unit coupling, $\beta(y - x) = -\beta(x - y) = -1$ [Figs. 5(e) and 5(f), compare also Figs. 3(c) and 3(d)]. This fixed point also exists for $\alpha > 0$ when the coupling is sufficiently strong such that at the fixed point $f(x) < 1$ and both variables are still in the vicinity of the fixed points of the intrinsic dynamics. For $\alpha < 0$, the fixed point splits into a stable fixed point at $(-\arccos(1 + 2\alpha) + (1 + \alpha)/\beta, -\arccos(1 + 2\alpha)^T$ and a saddle at $(\arccos(1 + 2\alpha) + (1 + \alpha)/\beta, \arccos(1 + 2\alpha))^T$ [Figs. 5(g) and 5(h)]. The same fixed points also exist for flipped x and y variables due to the symmetry of the unperturbed system.

In the main text, we explain the non-divergent responses for large perturbation strengths ε for $\alpha = 0.1 > 0$ in terms of a "ghost" fixed point at $(1/\beta, 0)^T$ for $\beta < 1/\pi$, which is the position of the fixed points before annihilation at $\alpha = 0$. Figure 5 illustrates that indeed, despite the saddle-node bifurcation, the dynamical flow remains overall similar for the different choices of α, apart from the small region between the two fixed points emerging for $\alpha < 0$. This structure of the flow remaining from the asymmetric stable fixed point $(-\arccos(1 + 2\alpha) + (1 + \alpha)/\beta, -\arccos(1 + 2\alpha))^T$ enables the asymmetric hybrid responses in strongly driven systems.

REFERENCES

[1] G. Karlebach and R. Shamir, "Modelling and analysis of gene regulatory networks," Nat. Rev. Mol. Cell Biol. **9**, 770–780 (2008).
[2] X. Zhang and M. Timme, "Fluctuation response patterns of network dynamics—An introduction," Eur. J. Appl. Math. **34**, 429–466 (2023).
[3] X. Zhang, C. Ma, and M. Timme, "Vulnerability in dynamically driven oscillatory networks and power grids," Chaos **30**(6), 063111 (2020).
[4] B. Schäfer, C. Beck, K. Aihara, D. Witthaut, and M. Timme, "Non-gaussian power grid frequency fluctuations characterized by lévy-stable laws and superstatistics," Nat. Energy **3**, 119–126 (2018).
[5] S. H. Strogatz, "Exploring complex networks," Nature **410**, 268–276 (2001).
[6] S. Allesina and S. Tang, "Stability criteria for complex ecosystems," Nature **483**, 205–208 (2012).
[7] F. Stollmeier and J. Nagler, "Unfair and anomalous evolutionary dynamics from fluctuating payoffs," Phys. Rev. Lett. **120**, 058101 (2018).
[8] X. Zhang, S. Hallerberg, M. Matthiae, D. Witthaut, and M. Timme, "Fluctuation-induced distributed resonances in oscillatory networks," Sci. Adv. **5**, eaav1027 (2019).
[9] D.-H. Kim and A. E. Motter, "Fluctuation-driven capacity distribution in complex networks," New J. Phys. **10**, 053022 (2008).
[10] P. Ashwin, S. Wieczorek, R. Vitolo, and P. Cox, "Tipping points in open systems: Bifurcation, noise-induced and rate-dependent examples in the climate system," Philos. Trans. R. Soc. A **370**, 1166–1184 (2012).
[11] T. M. Lenton, H. Held, E. Kriegler, J. W. Hall, W. Lucht, S. Rahmstorf, and H. J. Schellnhuber, "Tipping elements in the Earth's climate system," Proc. Natl. Acad. Sci. U. S. A. **105**, 1786–1793 (2008).
[12] J. Krönke, N. Wunderling, R. Winkelmann, A. Staal, B. Stumpf, O. A. Tuinenburg, and J. F. Donges, "Dynamics of tipping cascades on complex networks," Phys. Rev. E **101**, 042311 (2020).
[13] C. M. Bender and S. A. Orszag, *Advanced Mathematical Methods for Scientists and Engineers I: Asymptotic Methods and Perturbation Theory* (Springer Science & Business Media, 2013).
[14] S. H. Strogatz, *Nonlinear Dynamics and Chaos: With Applications to Physics, Biology, Chemistry, and Engineering* (CRC Press, 2018).
[15] M. Thümler, M. Schröder, and M. Timme, "Nonlinear and divergent responses of fluctuation-driven systems," IFAC-PapersOnLine **55**, 254–259 (2022).
[16] U. Feudel, A. N. Pisarchik, and K. Showalter, "Multistability and tipping: From mathematics and physics to climate and brain—Minireview and preface to the focus issue," Chaos **28**, 033501 (2018).
[17] J. Zhu, R. Kuske, and T. Erneux, "Tipping points near a delayed saddle node bifurcation with periodic forcing," SIAM **14**, 2030–2068 (2015).
[18] M. S. Williamson, S. Bathiany, and T. M. Lenton, "Early warning signals of tipping points in periodically forced systems," Earth Syst. Dyn. **7**, 313–326 (2016).
[19] L. Perko, *Differential Equations and Dynamical Systems* (Springer Science & Business Media, 2013), Vol. 7.
[20] R. Kubo, "Statistical-mechanical theory of irreversible processes. I. General theory and simple applications to magnetic and conduction problems," J. Phys. Soc. Jpn. **12**, 570–586 (1957).
[21] D. Ruelle, "A review of linear response theory for general differentiable dynamical systems," Nonlinearity **22**, 855 (2009).
[22] M. Thümler and M. Timme, "Boosted fluctuation responses in power grids with active voltage dynamics," J. Phys. Complexity **4**, 025019 (2023).
[23] R. Nisbet and W. Gurney, "Population dynamics in a periodically varying environment," J. Theor. Biol. **56**, 459–475 (1976).
[24] J. Ma, Y. Xu, J. Kurths, H. Wang, and W. Xu, "Detecting early-warning signals in periodically forced systems with noise," Chaos **28**(11), 113601 (2018).
[25] M. Anvari, G. Lohmann, M. Wächter, P. Milan, E. Lorenz, D. Heinemann, M. R. R. Tabar, and J. Peinke, "Short term fluctuations of wind and solar power systems," New J. Phys. **18**, 063027 (2016).
[26] M. Anvari, E. Proedrou, B. Schäfer, C. Beck, H. Kantz, and M. Timme, "Data-driven load profiles and the dynamics of residential electricity consumption," Nat. Commun. **13**, 4593 (2022).
[27] M. Ghil, "The wind-driven ocean circulation: Applying dynamical systems theory to a climate problem," Discrete Contin. Dyn. Syst. A **37**, 189–228 (2017).